



CHALMERS
UNIVERSITY OF TECHNOLOGY

A nuanced understanding of the doping of poly(3,4-ethylenedioxythiophene) with tosylate

Downloaded from: <https://research.chalmers.se>, 2025-03-23 15:09 UTC

Citation for the original published paper (version of record):

Petsagkourakis, I., Kim, D., Modarresi, M. et al (2023). A nuanced understanding of the doping of poly(3,4-ethylenedioxythiophene) with tosylate. *Discover Materials*, 3(0).
<http://dx.doi.org/10.1007/s43939-023-00046-6>


N.B. When citing this work, cite the original published paper.

A nuanced understanding of the doping of poly(3,4-ethylenedioxythiophene) with tosylate

Ioannis Petsagkourakis¹  · Donghyun Kim²  · Mohsen Modarresi³  · Sam Rudd⁴  · Roya Rudd⁵  · Igor Zozoulenko^{6,7}  · Drew Evans⁸ 

Received: 1 May 2023 / Accepted: 17 May 2023

Published online: 26 May 2023

© The Author(s) 2023  OPEN

Abstract

The conducting polymer poly(3,4-ethylenedioxythiophene) (known as PEDOT) is routinely fabricated into doped thin films for investigation of its inherent properties as well as for a range of applications. Fabrication of PEDOT is often achieved via oxidative polymerisation, where the conducting polymer is polymerised and doped (oxidised) to yield a conductive polymer thin film. The oxidiser and the polymerisation temperature are two parameters that may influence the properties and performance of the resultant PEDOT thin film. In this study, the role of temperature for the chemical polymerisation of PEDOT using the oxidiser iron tosylate is investigated from a computational and experimental viewpoint. While computations of the doping energetics suggest increasing doping with increasing temperature, x-ray photoelectron spectroscopy of fabricated PEDOT thin films indicate doping is much more complicated. With the aid of computations of the spatial distribution functions for tosylate in PEDOT, experiments indicate that two different populations of tosylate anions exist in the PEDOT matrix. Their relative populations change as a function of the polymerisation temperature. Therefore, polymerisation temperature plays a critical role in tailoring the properties of PEDOT in pursuit of being fit-for-purpose for the desired application.

1 Introduction

Thin films of conducting polymers typically consist of individual conjugated polymer chains that are self-assembled into a combination of aggregated, crystalline and/or amorphous domains. Counterions are often incorporated into the polymer material resulting in oxidation of the conjugated backbone of the polymer (creation of charge carriers). These charge carriers can move along the π -bonded structure of an individual polymer chain as well as hop between neighbouring chains—resulting in an electrically conducting polymer. The insertion of counterions into the polymer material is commonly referred to as doping. The process of doping, and its influence on, a conducting polymer is the subject of many fundamental studies and represents the key mechanism for many applications (OECT [1, 2], electrochromic [3, 4], sensors [5–7], etc.).

✉ Drew Evans, drew.evans@unisa.edu.au | ¹Division of Smart Hardware, Unit of Bio-and-Organic Electronics, Department of Digital Systems, RISE Research Institutes of Sweden, Sodra Grytsgatan 4, 60221 Norrköping, Sweden. ²Applied Chemistry, Department of Chemistry and Chemical Engineering, Chalmers University of Technology, 412 96 Gothenburg, Sweden. ³Department of Physics, Faculty of Science, Ferdowsi University of Mashhad, Mashhad, Iran. ⁴Airbridge Pty Ltd, Perth, WA 6000, Australia. ⁵Electro.Aero Pty Ltd, Perth, WA 6000, Australia. ⁶Laboratory of Organic Electronics, Department of Science and Technology, Linköping University, 60174 Norrköping, Sweden. ⁷Wallenberg Wood Science Center, Linköping University, 60174 Norrköping, Sweden. ⁸Future Industries Institute, UniSA STEM, University of South Australia, Adelaide, South Australia 5001, Australia.



When considering the family of conducting polymers currently available, poly(3,4-ethylenedioxythiophene) (PEDOT) stands out as one that is popularly studied [8]. This popularity is owed to the relative environmental stability and high electrical conductivity of PEDOT. By far the most common counterion for doping PEDOT is polystyrenesulfonate (PSS) [9]. This polymeric anion not only yields highly conductive polymer thin films but allows the inherently rigid insoluble PEDOT polymer to be solution processable (making thin film fabrication easy). Alternatively, the molecular anion *p*-toluenesulfonate (tosylate, Tos) is also utilised to fabricate doped PEDOT thin films [10–12]. Using iron(III) tosylate as an oxidiser, PEDOT doped with Tos (PEDOT:Tos) is fabricated using oxidative polymerisation. In this process EDOT monomer is polymerised into oligomers and polymer chains by reduction of the iron(III) to iron(II), while the presence of the Tos counterion affords doping of the resultant PEDOT all in the same process. In practice this is achieved by making an initial oxidant solution containing iron(III) tosylate in an alcohol solvent (such as *n*-butanol), subsequently mixing EDOT monomer into the solution at a given molar ratio to the oxidiser, and then coating onto a substrate. The coated substrate is heated to a set temperature and held for a time period to reach the desired film thickness/properties. Once cooled and washed (to remove residual and/or unreacted chemicals), the PEDOT:Tos coated substrate can be interrogated further.

To control the polymerisation process, researchers have explored a wide range of variations or modifications to the abovementioned method. Two variations are (i) adding other chemicals to the oxidant solution, and (ii) changing the temperature of the polymerisation process. Studies of de Leeuw et al. [10] and subsequently Winther-Jensen et al. [13, 14] explored the use of base inhibitor additives to raise the pH of the oxidant solution to avoid undesirable acidic side reactions of EDOT. These research efforts have led to the use of high pKa chemicals such as pyridine as common additives in the oxidant solution. Alternatively, Fabretto and co-workers [15, 16] introduced non-ionic copolymers to the oxidant solution to coordinate with the iron(III) and primarily inhibit the crystallisation of the oxidant (and subsequently template the growth of the PEDOT thin films). The use of pyridine or non-ionic copolymer as additives in the oxidant solution have become common place for the fabrication of highly conductive PEDOT:Tos thin films.

In this study the influence of polymerisation temperature on the chemical polymerisation of PEDOT:Tos is investigated. Firstly, using Density Functional Theory the change in Gibbs free energy upon doping of PEDOT oligomers is computed. The suggestion that increasing temperature results in increased doping level is then experimentally tested. Thin films of PEDOT:Tos are prepared from oxidant solutions containing no additive, pyridine, or copolymer, at temperatures ranging from 35 to 125 °C. X-ray photoelectron spectroscopy is used to determine the doping level for each PEDOT:Tos sample. Interestingly the doping of PEDOT appears more involved than first thought with two doping states observed. Computation of the spatial distribution function for Tos relative to the PEDOT chains/crystallites verifies that Tos can be located at one of two different positions relative to the PEDOT chains. Changing the polymerisation temperature changes the relative amounts of the two doped states, while the total level increases as suggested by computations. These results highlight that two discrete populations of Tos exist within doped PEDOT—with the polymerisation temperature having influence on the relative proportion of these doped states. It is envisaged that this impacts on the way in which PEDOT is then integrated into applications that rely on its doping, such as OECTs and electrochromic devices.

2 Materials and methods

2.1 Materials

The raw materials for the PEDOT:Tos polymerisation, 3,4-ethylenedioxythiophene (EDOT), *n*-butanol, pyridine, ethanol, PEG-PPG-PEG triblock copolymer (P123, 5800 Da.) were purchased from Sigma-Aldrich. The oxidant solution Clevios CB54, 54 wt.% iron tosylate in *n*-butanol, was purchased from Heraeus.

2.2 Methods

For the no additive oxidant, the Clevios CB54 was diluted to 40% w/w with *n*-butanol and stirred for 12 h in ambient conditions. For the pyridine-based oxidant, the Clevios CB54 was also diluted to 40% w/w with *n*-butanol, stirred for 12 h in ambient conditions, and 3% v/v pyridine was added with a further 12 h of stirring in ambient conditions. For the triblock copolymer-based oxidant, 23% w/w PEG-PPG-PEG triblock copolymer was added directly to the CB54 solution. The molar ratio of triblock copolymer to iron tosylate was 1:5. The new solution was stirred at 70 °C for 30 min. All oxidant solutions (with and w/o additive) were stored in a fridge before their usage in the polymerisation procedure. In-situ wet chemical polymerisation was used to deposit and polymerise PEDOT:Tos, as reported elsewhere [16]. 3.3 µl of the monomer were

added to 100 μl of the oxidant solution (with or w/o additive) and the mixture was stirred for 10–20 s. The EDOT/oxidant mixture was subsequently spin-coated on cleaned glass substrates (1500 rpm, 30 s, 800 rpm/s). After spin-coating, the films/substrate were positioned on a hot plate with varying temperatures based on our study, for 15 min. After the annealing step of 15 min a washing procedure followed so as to remove any unreacted oxidant/monomers; 5 min in n-butanol, then 5 min in n-butanol and finally 5 min in ethanol. Eventually, the films were dried with pressurised air.

As a reference sample, vapour phase polymerisation (VPP) was used for a PEG-PPG-PEG oxidant solution using a mixture of n-butanol and ethanol as the solvent [15, 17]. The VPP process was conducted at 25C, with the EDOT monomer heated to 35C in a vacuum chamber set to 45 mbar (VD115L, Binder).

2.3 Characterisation

XPS Instrumental calibration: All spectra were acquired using a Kratos AXIS Supra + photoelectron spectrometer. The X-ray source used was Al monochromatic K α (energy 1486.6 eV). Power output of the X-ray source was 225 W obtained by using source parameters 15 kV and 15 mA. The analysis chamber vacuum during spectral acquisition was 2×10^{-9} Torr. The charge neutralizer (Kratos) was used with neutralizer parameters: filament current 0.38 A, charge balance 0.67 V and filament bias 0.67 V. Instrument calibration was performed with gold and copper. The work function was set to -4.5 V giving an Au 4f $_{7/2}$ binding energy position of 84.03 eV. The spectrometer dispersion was set so that Cu 2p $_{3/2}$ was located at the binding energy of 932.69 eV. Instrument calibration procedure was carried out according to AS ISO 1547:2006-Surface chemical analysis-X-ray photoelectron spectrometers-calibration of spectrometer energy scale. This instrument calibration gave a metallic Ag 3d $_{5/2}$ peak located at 368.26 eV. All experimental spectra were collected over a rectangular analysis area with dimensions 300 \times 700 μm . Wide scan spectra were collected using pass energy of 160 eV. Narrow scan spectra were collected with a pass energy of 20 eV. Experimental spectra were charge corrected to adventitious carbon located at 285.0 eV. All spectra were analyzed using CasaXPS version 2.3.18PR1.0 (Casa Software Ltd, Wilmslow, Cheshire, UK).

Experimental XPS: The spectral shape of the C 1s, S 2p and O 1s were aligned with C–C (hydrocarbon) peak at 285.0 eV. In the S 2p spectra, three doublets were used for fitting with the hybridization of the 2p orbital at 1.2 eV and the area of S 2p $_{1/2}$ being half that of S 2p $_{3/2}$ respectively [18]. An asymmetric line shape was used for fitting the S 2p spectra of the PEDOT chain, for the doublet in the range of 163 to 166 eV. This has been performed previously by Zotti et al. [19] and defines the metallic behavior of the delocalized positive charges across the polymer chains. Two doublets were fitted in the 166 to 171 eV range to account for the two populations of Tos. The positions of these component peaks is informed by the deconvolution presented by Zotti et al. [19]. The doublet at 167.3 and 168.5 eV is assigned to S 2p $_{3/2}$ and 2p $_{1/2}$ of one proposed population of Tos. The doublet at 168.8 and 170 eV is assigned to S 2p $_{3/2}$ and 2p $_{1/2}$ of the other proposed population of Tos. The doping level of anions per EDOT repeat unit (or number of EDOT repeat units per 1 anion) was calculated by summation of the atomic percentage of anions relative to S in EDOT. Component peak fitting of the C 1s and O 1s follow the fitting parameters defined by Sethumadhavan et al. [17].

Electrical characterizations of PEDOT:Tos thin films were performed using a Kethley 2400 connected to a 4-point probe Signatone Pro4 S-302 measurement setup. The sheet resistance of the films was extracted upon measuring. A surface profilometer (Dektak 3st Veeco) was used to measure the thickness of the films. The electrical conductivity of the PEDOT films was then calculated as the inverse multiplication of the sheet resistance and the thickness.

2.4 Computations

Using Density Functional Theory (DFT), we calculated the Gibbs Energies of PEDOT $_N$ (chain length $N=6$ and 12) with respect to doping (oxidation) level (C_{ox}) ranging from 0 to 50% at 298 and 323K as per the doping step of in-situ oxidative polymerization of PEDOT with Iron Tosylate as oxidant. Note that the doping level of PEDOT denotes the ratio between the number of positive charges (n_i) and the number of EDOT monomer units in a PEDOT chain (i.e., $C_{\text{ox}}=50\%$ corresponds to $n_i=3$ and 6 for PEDOT $_6$ and PEDOT $_{12}$ respectively). DFT simulations were carried out at a level of wb97xd [20] functional and 6-31G(d) [21] basis set as implemented in Gaussian 09 package. The effect of solvent effect was accounted for implicitly, via the polarizable continuum model reference. [22].

The oxidation of oligomers occurs as below [12],



where PEDOT_N^{n+} stands for N -oligomer of PEDOT with n positive charges, and Tos^- is a negatively charged tosylate molecule. The change of the Gibbs energy after doping of the oligomer is calculated as below,

$$\Delta G = \sum G_{\text{products (doped PEDOT)}} - \sum G_{\text{reactants (neutral PEDOT)}} \quad (2)$$

where reactants and products are those defined in Eq. (1). For example, for the case of PEDOT oligomer with two charges the reactants and products are respectively: reactants: $\text{PEDOT}_N^0 + 2\text{Fe}^{3+}(\text{Tos}^-)_3$, products: $\text{PEDOT}_N^{2+} + 2\text{Tos}^- + 2\text{Fe}^{2+}(\text{Tos}^-)_2$. Further details on the calculations including accounting for spin multiplicities and performing geometry optimization, are described in our previous study in which the Gibbs energies were calculated at 373 K [12].

2.5 The coarse-grained molecular dynamics simulation

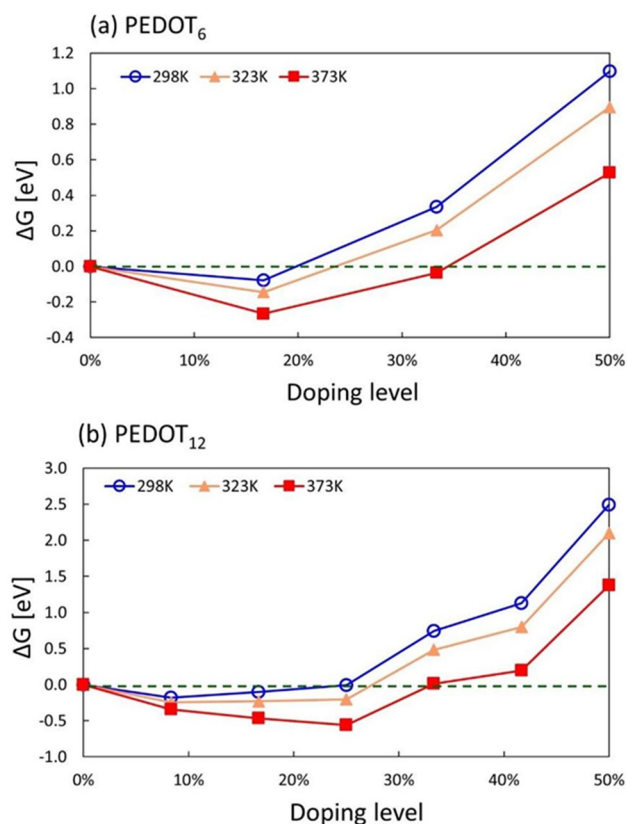
A coarse-grained Martini 2 molecular dynamics simulation of PEDOT:Tos is performed in the isothermal–isobaric (NPT) ensemble to investigate the distribution of Tos molecules around PEDOT chains. Our simulation closely follows the one presented in our previous paper [17]. The simulation starts with a solution of PEDOT, Tos, and water molecules. In the initial solution, PEDOT and Tos molecules are distributed randomly in the whole simulation box. The system is then filled with polarizable Martini water molecules. The Martini 2 coarse-grained models for PEDOT and Tos are developed and explained in our previous works [17]. The molecular dynamics (MD) simulations start with an energy minimization and an equilibration step. In the equilibration step a restraint is applied for 50 ns to the polymer matrix and water molecules are free to fill the space under $T = 300$ K and $P = 1$ atm. The production run for the solution is performed for 500 ns. The solution is dried by random removing water molecules from the simulation box in 50 successive steps. In each step, two percent of the remaining water molecules are removed followed by a 10 ns equilibration of water molecules and a 20 ns production run. The total simulation time for water evaporation is 1.5 μs in the NPT ensemble. The final dried film is used to plot the spatial distribution functions (SDFs) by using the ViaMD analysis package [18]. All the molecular dynamics simulations are performed by using the GROMACS computational package [19].

3 Results and discussion

Previous computational work explored the doping level as a function of PEDOT chain length—giving supporting evidence to the preferred 33% doping level in PEDOT [12]. (It is worth noting that a doping level of 33% typically reported in oxidized PEDOT was explained by Kim and Zozoulenko by the change of the character of the bonds in the oligomers (aromatic to quinoid) that occurs at this oxidation level) [12]. Herein, computational work was undertaken to explore the effect of temperature during PEDOT polymerisation on the final doping level of PEDOT:Tos. The change of the calculated Gibbs energy (ΔG) for PEDOT oligomers as a function of the doping level (C_{ox}) with respect to the Gibbs energy of undoped oligomers ($C_{\text{ox}} = 0$) is shown in Fig. 1 for different temperatures $T = 298, 323$ and 373 K (Fig. 1). Negative value of ΔG means that doping is thermodynamically favourable, whereas positive ΔG corresponds to the unfavourable process. For $T = 373$ K, ΔG turns to zero (passing from negative to positive values) at the doping level of $C_{\text{ox}} = 33\%$ for both chain lengths $N = 6$ and 12 , which defines the maximal doping level that can be reached at this temperature. (It is noteworthy that chain lengths of PEDOT is unknown because of its insolubility. Theoretical modelling suggests that PEDOT chains are rather short, $N = 6–12$) [20]. As temperature decreases, the maximal doping level (obtained from the condition $\Delta G = 0$) also decreases for both $N = 6$ and 12 ; for example, for $T = 298$ K and $N = 12$ the oligomer can be doped up to $C_{\text{ox}} = 25\%$. To summarize, this computational work suggests that increasing the polymerisation temperature would in turn increase the doping level of the final doped PEDOT.

To verify the computational results, experiments were conducted for fabricating PEDOT:Tos via chemical polymerisation at different temperatures. Three different oxidant solutions were employed; (i) no additive, (ii) base inhibitor (pyridine) added, and (iii) non-ionic triblock copolymer. Samples were prepared by chemical polymerisation. This entails spin coating a solution containing the oxidant (plus any additive) and EDOT monomer onto substrates, and then placing on a hot plate at the set temperature for 15 min. After this, each sample was washed using ethanol as per the protocol described in the Materials and Methods section.

Fig. 1 The change of Gibbs Free Energy (eV) at 298 (blue open circles), 323 (orange filled triangles), and 373K (red filled squares) upon doping of PEDOT oligomers at doping levels from 0 to 50% for (a) PEDOT₆ and (b) PEDOT₁₂



X-ray Photoelectron Spectroscopy (XPS) was used to characterise the doping level of Tos in the PEDOT. The fine scan of the S 2p orbital was used to define the relative amount of Tos and PEDOT in the top 15 to 30 nm of the sample (examples provided Fig. 2). From these fine scans, in all cases, three S environments were observed; The S of PEDOT (doublet in 163–166 eV), the S of one Tos environment ('Tos 1' doublet in 166–170 eV) typical for PEDOT:Tos, and a second population of Tos ('Tos 2', 167–171 eV). These three S environments are in agreement with the studies of Zotti et al. studying PEDOT doped with Tos or PSS [19], where the 'Tos 2' population is assigned as protonated Tos. More specifically, Zotti et al. reported the presence of protonated dopant, especially Tos, in the final PEDOT films.

From the S 2p fine scans, the total amount of Tos was determined, as a percentage with respect to the PEDOT amount. As shown in Fig. 3a, there is a general trend that the increasing polymerisation temperature results in an increasing total population of Tos in PEDOT. This is irrespective of the additive (or not) within the oxidant solution. In relation to the computational results presented above, there appears to be agreement that increasing the temperature during polymerisation yields an increasing amount of dopant in PEDOT. Further to this, the additional 'PEG-PPG-PEG' copolymer data point at 25 °C is a reference PEDOT:Tos prepared via vapour phase polymerisation with the oxidant layer at 25 °C. The agreement of this data point with the trend for the chemically polymerised samples suggests the mechanisms at play are generic to oxidative polymerisation (rather than the fabrication method itself).

In the work of Zotti et al., they elaborate on the role of Tos in the electropolymerisation of PEDOT [21]. They report that Tos acts as a proton scavenger in aprotic solvents such as acetonitrile. During polymerisation, when the relative concentration of EDOT is high then a significant number of protons are released, which then 'neutralise' Tos through protonation (therefore blocking Tos from over-oxidising oligomers and stopping polymerisation). This is a potential source of protonated Tos in the final PEDOT:Tos. For the study herein, the solvent is protic (n-butanol) and hence capable of participating in stabilisation of the PEDOT positive charge (carbocations) during polymerisation. The role of proton scavengers in protic solvents was previously explored, but in the context of trace water in the VPP process (no additive [15], and with added triblock copolymer [22]). To gain some insight into what this means for chemical polymerisation of PEDOT:Tos in n-butanol (with or without additives), the S 2p fine scans were inspected in closer detail. Upon closer interrogation of the Tos signal in the S 2p, it may be possible to follow the teachings of Zotti et al. and assign 'Tos 1' and 'Tos 2' as Tos that dopes PEDOT and protonated Tos, respectively [21]. As the polymerisation temperature increases the proportion of Tos doping PEDOT decreases, see Fig. 3b (conversely, the proportion of protonated Tos increases,

Fig. 2 Example XPS S 2p fine scan of PEDOT:Tos polymerised with **a** Pyridine at 30 C, and **b** Pyridine at 125 C. The doublet at 163.9 and 165.2 eV is assigned to S 2p_{3/2} (solid, blue) and 2p_{1/2} (dashed, blue) in PEDOT. The doublet at 167.3 and 168.5 eV is assigned to S 2p_{3/2} (solid, yellow) and 2p_{1/2} (dashed, yellow) of Tos population 1 ('Tos 1'). The doublet at 168.8 and 170 eV is assigned to S 2p_{3/2} (solid, green) and 2p_{1/2} (dashed, green) of Tos population 2 ('Tos 2'). The combined fitting envelope (dashed, black) and background (solid, black) are provided for reference to compare to the measured data (solid, red)

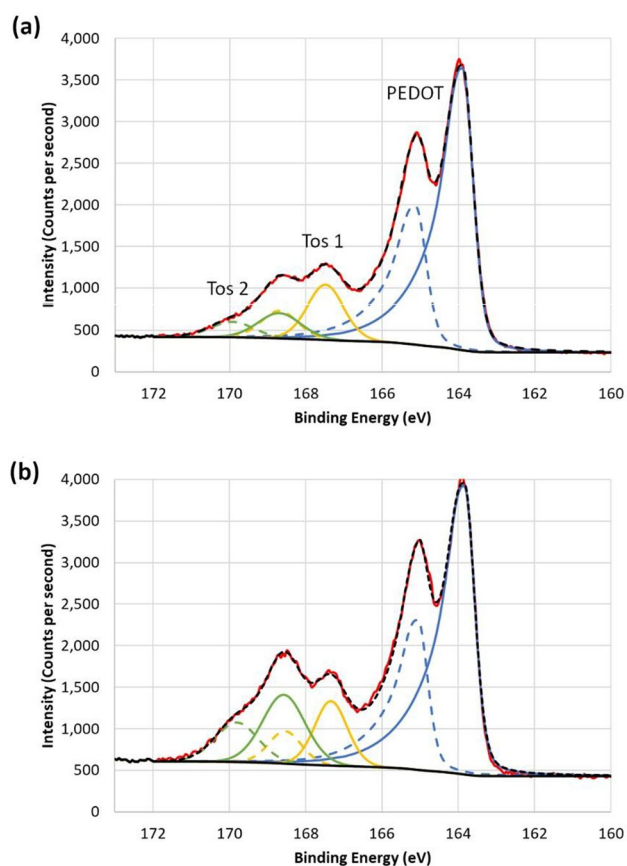
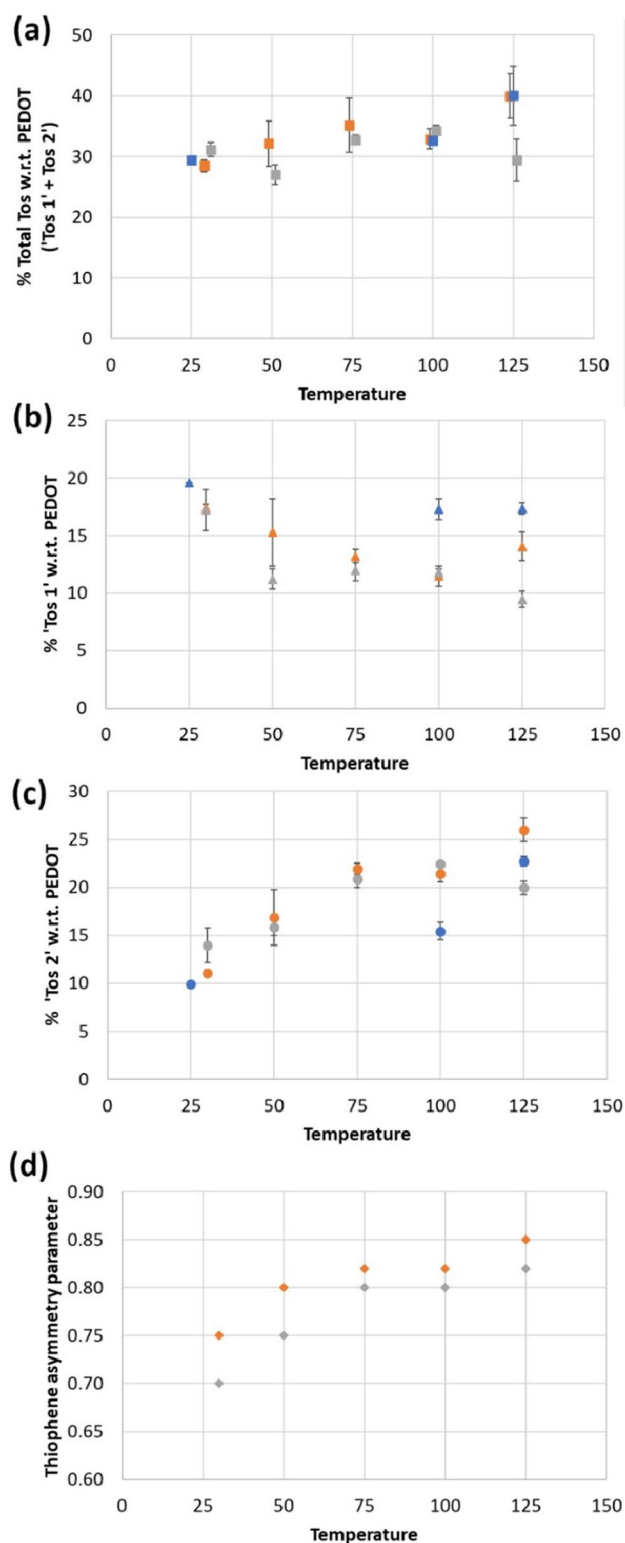


Fig. 3c). Following the rationale presented by Zotti et al. the % of protonated Tos in the final PEDOT is as an indicator of the relative efficiency for Tos to scavenge available protons in the protic solvent. One way to interpret Fig. 3 is that increasing the polymerisation temperature increases the % of Tos present in the final PEDOT film, and that Tos is more readily neutralised (protonated) at elevated temperatures. This appears to be independent of the additives (i.e. pyridine or co-polymer) present in the oxidant solution. However, a flaw in this interpretation is that protonated Tos is soluble in the solvents used to wash the samples. This should lead to negligible concentrations of residual protonated Tos in the final PEDOT:Tos films. Another indirect support of the absence of protonated Tos in PEDOT:Tos films is related to the fact that PEDOT:Tos films, in contrast to PEDOT:PSS films, do not intake water or exhibit detectable ionic conductivity when immersed in water [23]. (Note that the presence of water in the film is a prerequisite for the ionic conductivity) [17]. It was shown that ionic conductivity and water intake of PEDOT:PSS are caused by deprotonation of PSS facilitating water intake into the film [24]. Thus, if PEDOT:Tos had protonated Tos molecules, they would also de-protonate when the film is immersed in water, leading to a detectable ionic conductivity. This however is not seen experimentally.

An alternate hypothesis is that the two Tos populations observed in the S 2p fine scans are both electrostatic interactions of Tos but interacting with two different chemical environments within PEDOT. The electrostatic interaction of Tos may stabilise charge carriers on two discretely different chemical environments on the conjugated backbone of PEDOT. This is explained by the observable difference in the XPS binding energy of the respective doublets in the S 2p fine scan (Fig. 2). The higher binding energy doublet for 'Tos 2' signifies the S atom within the Tos has a relatively larger positive character (higher ionisation potential). This in turn indicates 'Tos 2' has a larger polarisation of the S–O bond in the sulfonate group relative to 'Tos 1'—rationalised by the assumption of a commensurate change in electrostatic interaction with PEDOT. Also, as the polymerisation temperature is changed there is a change in the lower binding energy doublet attributed to S in the thiophene ring of PEDOT. That is, the coefficient for asymmetry used to fit the thiophene S 2p_{3/2} and 2p_{1/2} doublet (Fig. 3d) must be increased as the polymerisation temperature is increased to achieve a good fit to the experimental XPS measurements. This is similar to the increasing asymmetry with increasing electrical conductivity seen for oxidised or reduced PEDOT:Tos [25]. The asymmetry has been previously reported as a qualitative means to probe charge carriers at or near the Fermi level [26]. The observation of

Fig. 3 Percentage of the Tos populations ('Tos 1' and 'Tos 2') relative to PEDOT as determined from the component peaks in the S 2p fine scan. **a** Total Tos, **b** 'Tos 1' population, and **c** 'Tos 2' population with respect to PEDOT. All data is presented with respect to the temperature of polymerisation (in °C) for no additive (grey), pyridine (orange), and triblock copolymer (blue) containing oxidant solutions. In **a** the data points have been offset by $-1\text{ }^{\circ}\text{C}$ (pyridine data) or $+1\text{ }^{\circ}\text{C}$ (no additive data) in the x-scale to make the overlapping data points visible. **d** The fitting parameter (x) for the asymmetric function $\text{SGL}(30)\text{T}(x)$ used to fit the S doublet of the thiophene S in the S 2p XPS fine scan



asymmetry in the S 2p doublet indicates that the S 2p orbitals of the S thiophene contribute to the density of states near the Fermi level, with increasing asymmetry correlating with an increasing contribution to the density of states. This is in agreement with Folmer and de Boer's interpretation of asymmetric S 2p peaks in metallic CuS_2 [26]. By virtue of this, we hypothesise that 'Tos 2' is a population that has a stronger interaction with (possibly based on proximity to) the thiophene S in PEDOT compared with 'Tos 1'.

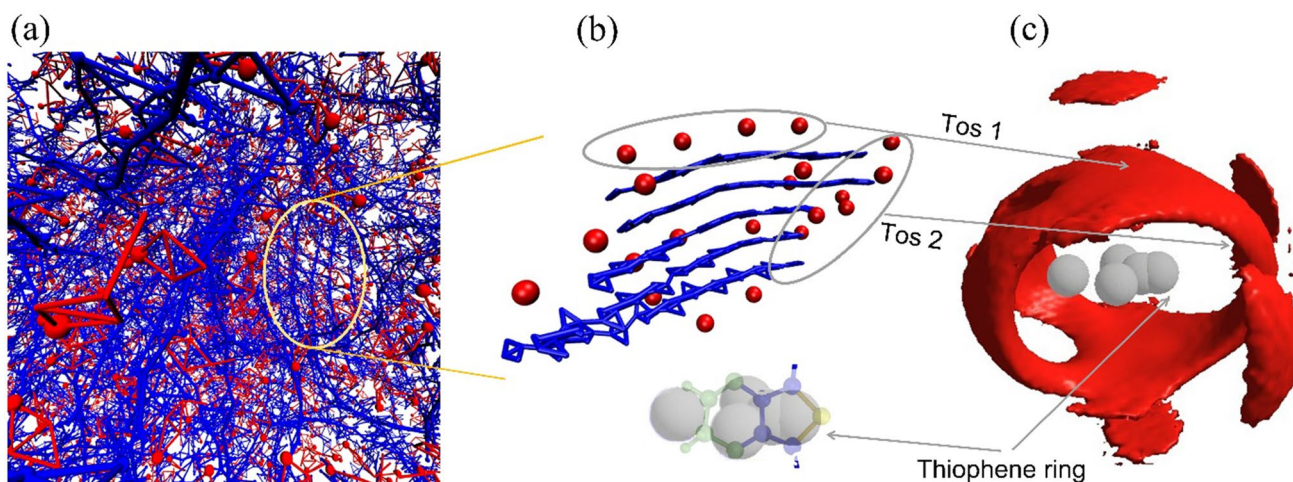


Fig. 4 **a** The snapshot of the coarse-grained molecular dynamics simulation of the dried PEDOT:Tos film. The PEDOT chains and Tos molecules are in blue and red colour, respectively. For a better presentation, the PEDOT skeleton is visualized by connecting the beads in the coarse-grained MD model. **b** A typical PEDOT stacking with surrounding Tos molecule (For Tos molecules, only a sulfonate group is visualized). **c** The calculated SDF for Tos molecules around a PEDOT monomer. 'Tos 1' and 'Tos 2' refer to two tosylate populations, see text for details

In order to further solidify this hypothesis, computational microscopy in the form of molecular dynamics simulations were performed, so as to determine the spatial distribution functions (SDF) of Tos relative to PEDOT (Fig. 4). Note that a detailed discussion of the calculated morphology and ion diffusion in PEDOT:TOS was given in Modarresi et al. [17] Fig. 4a, b shows a snapshot of the simulated morphology of the final dried PEDOT:Tos film. The PEDOT chains are stacked into small crystallites and surrounded by Tos molecules that are attracted by the Coulomb force to the positive charges in PEDOT chains. The SDF for Tos (see Fig. 4c) reveals that two distinct locations of Tos relative to the PEDOT chains can be identified. The first population of Tos molecules (Tos 1) surrounds the side of PEDOT crystallites, in a π -anion configuration. The second population of Tos molecules (Tos 2) is situated in proximity of the thiophene S atom of the PEDOT chains. It should be noted that while the Tos 1 molecules surrounding the crystallite stand in the π -direction of PEDOT, they are not intercalated within the π - π stacking structure of PEDOT chains as suggested for very high doping levels [27] or other anions [28]. Such a case of Tos within π - π stacking should have led to changes in π - π distance and thus to the electrical conductivity of the PEDOT:Tos films. However, the electrical conductivity of the PEDOT:Tos samples is reasonably constant as a function of temperature since PEDOT:Tos without additives had an electrical conductivity of 220 ± 6 S/cm at 30 °C, 320 ± 10 S/cm at 100 °C, and 240 ± 5 S/cm at 125 °C. Therefore, these simulations support the XPS spectra presented in Fig. 2, and the evidence of two electrostatically discrete populations of Tos in connection to the PEDOT chains.

4 Conclusion

In PEDOT:Tos there is evidence for two discrete populations of Tos which are spatially different with respect to the PEDOT chains and electrostatically interact in two discretely different interactions. These two populations are observable via XPS (S 2p fine scans). SDFs computed for Tos in PEDOT:Tos lend support to this interpretation. When considering the experimental fabrication of PEDOT:Tos films, the temperature of polymerisation has been shown to modify the relative proportion of Tos in the two different states. This is hypothesised to arise from the polymerisation temperature influencing the molecular scale arrangement of PEDOT chains (π - π stacking and crystallites) and the relative position of Tos. In term of total doping, agreement is shown between Gibbs free energy calculations and experiments that increasing polymerisation temperature leads to increased total doping levels. All of these results and interpretations combine to give a more nuanced understanding of doped PEDOT:Tos, which will have ramifications for how PEDOT:Tos is utilised in applications. We envision that our findings will solidify the understanding behind many of the electro-optical, electro-chemical and electrocatalytic behaviours of doped conducting polymers.

Acknowledgements IZ acknowledges financial support from the Wallenberg Wood Science Center and Knut and Alice Wallenberg Foundation (project “H2O2”). The computations were performed on resources provided by the National Academic Infrastructure for Supercomputing in Sweden (NAISS) at NSC, HPC2N and PDC. The authors acknowledge the facilities, scientific and technical assistance of Microscopy Australia at the University of South Australia, a facility that is co-funded by the University of South Australia, and the State and Federal Governments. The authors acknowledge the informative discussions with Prof. David Martin during the early stages of this research project.

Author contributions IP, SR, RR, and DE conducted the experimental work. DK, MM and IZ conducted the simulation and computation work. IP, IZ and DE wrote the main manuscript text, and all authors prepared the Fig. 1, 2, 3 and 4. All authors read and approved the final manuscript.

Data availability The datasets generated during and/or analysed during the current study are available from the corresponding author on reasonable request.

Declarations

Competing interests The authors declare no competing interests.

Open Access This article is licensed under a Creative Commons Attribution 4.0 International License, which permits use, sharing, adaptation, distribution and reproduction in any medium or format, as long as you give appropriate credit to the original author(s) and the source, provide a link to the Creative Commons licence, and indicate if changes were made. The images or other third party material in this article are included in the article's Creative Commons licence, unless indicated otherwise in a credit line to the material. If material is not included in the article's Creative Commons licence and your intended use is not permitted by statutory regulation or exceeds the permitted use, you will need to obtain permission directly from the copyright holder. To view a copy of this licence, visit <http://creativecommons.org/licenses/by/4.0/>.

References

1. Zeglio E, Inganäs O. Active materials for organic electrochemical transistors. *Adv Mater.* 2018;30(44):1800941.
2. Rivnay J, Inal S, Salleo A, Owens RM, Berggren M, Malliaras GG. Organic electrochemical transistors. *Nat Rev Mater.* 2018;3(2):1–14.
3. Mortimer RJ. Electrochromic materials. *Chem Soc Rev.* 1997;26(3):147–56.
4. Rosseinsky DR, Mortimer RJ. Electrochromic systems and the prospects for devices. *Adv Mater.* 2001;13(11):783–93.
5. Mokhtar SMA, Alvarez de Eulate E, Yamada M, Prow TW, Evans DR. Conducting polymers in wearable devices. *Med Dev Sens.* 2021;4(1):e10160.
6. Sethumadhavan V, Rudd S, Switalska E, Zuber K, Teasdale P, Evans D. Recent advances in ion sensing with conducting polymers. *BMC Mater.* 2019;1(1):1–14.
7. Bobacka J, Ivaska A, Lewenstam A. Potentiometric ion sensors. *Chem Rev.* 2008;108(2):329–51.
8. Elschner A, Kirchmeyer S, Lovenich W, Merker U, Reuter K. PEDOT: principles and applications of an intrinsically conductive polymer, CRC press: 2010. <https://doi.org/10.1201/b10318>
9. Jonas F, Morrison J. 3, 4-polyethylenedioxythiophene (PEDT): Conductive coatings technical applications and properties. *Synth Met.* 1997;85(1–3):1397–8.
10. De Leeuw DM, Kraakman P, Bongaerts P, Mutsaers C, Klaassen D. Electroplating of conductive polymers for the metallization of insulators. *Synth Met.* 1994;66(3):263–73.
11. Evans D. Understanding PEDOT doped with tosylate. *Chem Commun.* 2022;58(29):4553–60.
12. Kim D, Zozoulenko I. Why is pristine PEDOT oxidized to 33%? A density functional theory study of oxidative polymerization mechanism. *J Phys Chem B.* 2019;123(24):5160–7.
13. Winther-Jensen B, West K. Vapor-phase polymerization of 3, 4-ethylenedioxythiophene: a route to highly conducting polymer surface layers. *Macromolecules.* 2004;37(12):4538–43.
14. Winther-Jensen B, Breiby DW, West K. Base inhibited oxidative polymerization of 3, 4-ethylenedioxythiophene with iron (III) tosylate. *Synth Met.* 2005;152(1–3):1–4.
15. Zuber K, Fabretto M, Hall C, Murphy P. Improved PEDOT conductivity via suppression of crystallite formation in Fe (III) tosylate during vapor phase polymerization. *Macromol Rapid Commun.* 2008;29(18):1503–8.
16. Fabretto MV, Evans DR, Mueller M, Zuber K, Hojati-Talemi P, Short RD, Wallace GG, Murphy PJ. Polymeric material with metal-like conductivity for next generation organic electronic devices. *Chem Mater.* 2012;24(20):3998–4003.
17. Modarresi M, Franco-Gonzalez JF, Zozoulenko I. Morphology and ion diffusion in PEDOT: Tos. A coarse grained molecular dynamics simulation. *Phys Chem Chem Phys.* 2018;20(25):17188–98.
18. Skånberg R, Linares M, König C, Norman P, Jönsson D, Hotz I, Ynnerman A. In *VIA-MD: visual interactive analysis of molecular dynamics*, MolVa@EuroVis, 2018; pp 19–27.
19. Berendsen H, Hess B, Lindahl E, Van Der Spoel D, Mark A, Groenhof G. GROMACS: fast, flexible, and free. *J Comput Chem.* 2005;26(16):1701–18.
20. Kim D, Franco-Gonzalez JF, Zozoulenko I. How long are polymer chains in poly (3, 4-ethylenedioxythiophene): Tosylate Films? An insight from molecular dynamics simulations. *J Phys Chem B.* 2021;125(36):10324–34.

21. Zotti G, Zecchin S, Schiavon G, Louwet F, Groenendaal L, Crispin X, Osikowicz W, Salaneck W, Fahlman M. Electrochemical and XPS studies toward the role of monomeric and polymeric sulfonate counterions in the synthesis, composition, and properties of poly (3, 4-ethylenedioxythiophene). *Macromolecules*. 2003;36(9):3337–44.
22. Mueller M, Fabretto M, Evans D, Hojati-Talemi P, Gruber C, Murphy P. Vacuum vapour phase polymerization of high conductivity PEDOT: Role of PEG-PPG-PEG, the origin of water, and choice of oxidant. *Polymer*. 2012;53(11):2146–51.
23. Delavari N, Gladisch J, Petsagkourakis I, Liu X, Modarresi M, Fahlman M, Stavrinidou E, Linares M, Zozoulenko I. Water intake and ion exchange in PEDOT: Tos films upon cyclic voltammetry: experimental and molecular dynamics investigation. *Macromolecules*. 2021;54(13):6552–62.
24. Modarresi M, Mehandzhiyski A, Fahlman M, Tybrandt K, Zozoulenko I. Microscopic understanding of the granular structure and the swelling of PEDOT: PSS. *Macromolecules*. 2020;53(15):6267–78.
25. Rudd S, Mahjoub R, Switalska E, Bassell C, Schmerl N, Cavallaro A-A, Stanford N, Evans DR. Surface doping in poly (3, 4-ethylenedioxythiophene)-based nanoscale films: insights for polymer electronics. *ACS Appl Nano Mater*. 2022;5(9):12143–53.
26. Folmer J, De Boer D. XPS core level line shapes in metallic compounds: a probe for the nature of the electrons at the Fermi level. *Solid State Commun*. 1981;38(12):1135–8.
27. Rehmen J, Zuber K, Modarresi M, Kim D, Charrault E, Jannasch P, Zozoulenko I, Evans D, Karlsson C. Structural control of charge storage capacity to achieve 100% doping in vapor phase-polymerized PEDOT/tosylate. *ACS Omega*. 2019;4(26):21818–26.
28. Rudd S, Franco-Gonzalez JF, Kumar Singh S, Ullah Khan Z, Crispin X, Andreasen JW, Zozoulenko I, Evans D. Charge transport and structure in semimetallic polymers. *J Polym Sci B*. 2018;56(1):97–104.

Publisher's Note Springer Nature remains neutral with regard to jurisdictional claims in published maps and institutional affiliations.